Antibody Based Surgical Imaging and Photodynamic Therapy for Cancer

de Boer, Esther

4

Safety and Tumor-specificity of Cetuximab-IRDye800 for Surgical Navigation in Head and Neck Cancer

E. L. Rosenthal,[1] J. M. Warram,[1] **E. de Boer**,[1,2] T. K. Chung,[1] M. L. Korb,[3] M. S. Brandwein-Gensler,[4] T. V. Strong,[5] C. E. Schmalbach,[1] A. B. Morlandt,[6] G. Agarwal,[1] Y. E. Hartman,[1] W. R. Carroll,[1] J. S. Richman,[3] L. K. Clemons,[1] L. M. Nabell[5] and K. R. Zinn[7]

1. Division of Otolaryngology, University of Alabama at Birmingham, USA.
2. Department of Surgery, University Medical Center Groningen, University of Groningen, The Netherlands.
3. Division of General Surgery, Department of Surgery, University of Alabama at Birmingham, USA.
4. Division of Anatomic Pathology, Department of Pathology, University of Alabama at Birmingham, USA.
5. Division of Hematology/Oncology, University of Alabama at Birmingham, USA.
6. Department of Oral & Maxillofacial Surgery, University of Alabama at Birmingham, USA.
7. Division of Advanced Medical Imaging, Department of Radiology, University of Alabama at Birmingham, USA.

Published in **Clinical Cancer Research, August 2015,** 21(16):3658-66.
DOI: 10.1158/1078-0432

ABSTRACT

PURPOSE

Positive margins dominate clinical outcomes after surgical resections in most solid cancer types including head and neck squamous cell carcinoma. Unfortunately, surgeons remove cancer in the same manner they have for a century with complete dependence on subjective tissue changes to identify cancer in the operating room. To effect change, we hypothesize that epidermal growth factor receptor (EGFR) can be targeted for safe and specific real-time localization of cancer.

EXPERIMENTAL DESIGN

A dose escalation study of cetuximab conjugated to IRDye800 was performed in patients (n=12) undergoing surgical resection of squamous cell carcinoma arising in the head and neck. Safety and pharmacokinetic data were obtained out to 30 days post-infusion. Multi-instrument fluorescence imaging was performed in the operating room and in surgical pathology.

RESULTS

There were no grade 2 or higher adverse events attributable to cetuximab-IRDye800. Fluorescence imaging with an intraoperative, wide-field device successfully differentiated tumor from normal tissue during resection with an average tumor-to-background ratio of 5.2 in the highest dose range. Optical imaging identified opportunity for more precise identification of tumor during the surgical procedure and during the pathological analysis of tissues ex-vivo. Fluorescence levels positively correlated with EGFR levels.

CONCLUSION

We demonstrate for the first time that commercially available antibodies can be fluorescently labeled and safely administered to humans to identify cancer with sub-millimeter resolution, which has the potential to improve outcomes in clinical oncology.

INTRODUCTION

The primary treatment for many solid cancers remains surgical resection with negative margins which requires accurate identification of cancer in real-time. Patients with squamous cell carcinoma arising in the head and neck region often undergo surgical extirpation as part of their primary or salvage treatment.[1] The incidence of involved or close surgical margins approaches 40% on histopathological review,[2,3] resulting in a significantly worse outcome.[4] Positive margins rates have not significantly changed over the past several decades because surgeons cannot successfully differentiate normal and diseased tissue.

Failure to identify residual disease in this patient population is not surprising considering that the surgeon must rely on non-specific visual changes and manual palpation of subtle irregularities to guide successful excision. The most common method of intraoperative margin control remains frozen section analysis, however this technique is time intensive and can sample only a small fraction of the wound bed. To address the need for intraoperative cancer identification, conventional anatomical imaging modalities have been adopted for use in the operating room. Unfortunately, these are neither real-time nor tumor specific, and do not allow surgical field of view. Cancer-specific navigation has been successfully introduced in glioma surgery with improvement in outcomes,[5-7] but this strategy lacks specificity and applicability to other cancer types.[8] Adapting therapeutic antibodies for intraoperative cancer imaging leverages the known safety profile of the antibody to facilitate the clinical translation of the technique for surgical navigation in oncology.[9,10]

Based on extensive preclinical data establishing the feasibility of antibody-based imaging,[11,12] we hypothesize that fluorescently labeled anti-epidermal growth factor receptor (EGFR) antibody would be safe and enable detection of squamous cell cancer in humans.[13,14] Over 90% of head and neck tumors are known to overexpress EGFR.[15-17] We selected IRDye800 for optical labeling for this study because previous rodent studies show a lack of toxicity,[18] the dye is manufactured under conditions suitable for human use, and preclinical studies in non-human primates comparing cetuximab-IRDye800 to cetuximab alone showed no clinically significant toxicities.[19]

The safety and tumor specificity of optically labeled antibodies has not been previously assessed in humans. To this end, we evaluated escalating doses of cetuximab-IRDye800 in a phase I clinical trial to localize microscopic fragments of cancer during operative and pathological tumor assessment (Figure 1).

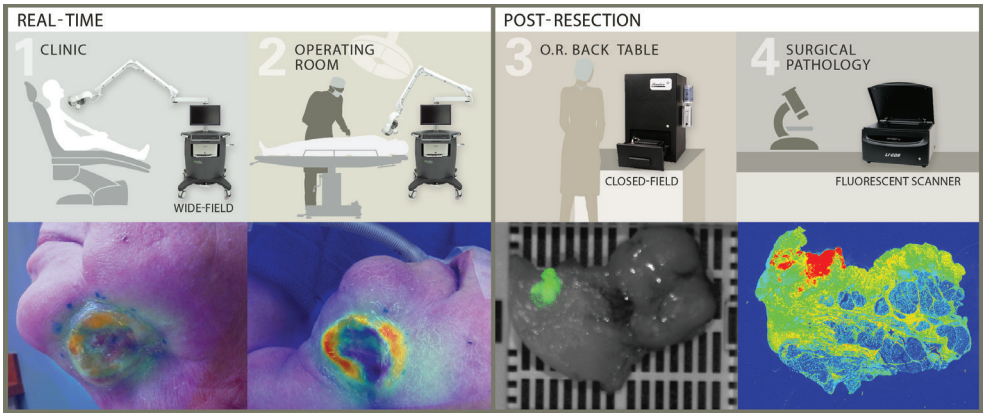

Figure 1 Trial Imaging Workflow. *Real-time imaging was performed with a wide-field near-infrared imaging system in the clinic on (1) Day 0, 1, and in the (2) operating room on day 3 post cetuximab-IRDye800 infusion. (3) During post-resection processing, resected tissues were imaged with a closed-field near-infrared imaging system. (4) Following histologic preparation, a corresponding slide was imaged in surgical pathology using a fluorescence scanning system.*

METHODS

STUDY DESIGN

Patients scheduled to undergo surgical extirpation were identified in the otolaryngology clinic at the University of Alabama at Birmingham. Of the 14 individuals aged 40–84 years with biopsy proven squamous cell carcinoma of the head and neck that were evaluated for trial eligibility, 12 were enrolled. Patients were not enrolled if they had an allergic reaction to either a 10mg or 100mg test dose of unlabeled cetuximab. Karnofsky score of greater than 70% and normal electrolyte parameters were required. All patients were given informed consent and the UAB Institutional Review Board approved the study. The FDA approved the study protocol (NCT01987375) and the manufacturing process of the cetuximab-IRDye800 by the UAB Vector Production Facility as previously described.[19] Because this was a first in human study with the conjugated antibody, it was unknown whether immunological reaction may limit dosing and optimal tumor to background ratio. Sample size was based on traditional 3+3 phase I dose escalation model to identify the optimal tumor to background ratio. Consented patients meeting study criteria were admitted to the infusion center for study drug administration. A pretreatment dose of 10mg or 100mg unlabeled cetuximab was administered prior to the study drug to differentiate between a cetuximab reaction and a cetuximab-IRDye800 reaction. During and after cetuximab-IRDye800 infusion, hemodynamic measurements and ECG data were obtained. The escalating doses were based on the therapeutic dose of cetuximab (250mg/m^2). The first three patients (cohort 1) were given a microdose (1% of thera-

Table 1 - Patient characteristics

	#	Age	Sex	Cancer Origin	Tumor Site	Cancer Stage	Prior Chemo	Prior Radiation	Dye Dose (mg)	Procedure	Possibly/Probably Related Adverse Events
Cohort 1 2.5 mg/m^2	1	42	M	Oral Cavity	Lateral Tongue	T1, N2b	N	N	5.0	Partial Glossectomy with ND	Elevated AST (Grade 1)
	2	50	M	Cutaneous	Temple	T2, N1	N	Y	6.1	Wide Local Excision with ND and FF	Tumor Redness (Grade 1) Tumor Swelling (Grade 1)
	3	64	F	Oral Cavity	Floor of Mouth	T3, N0	N	N	4.4	Composite Resection with ND and FF	Sinus Bradycardia (Grade 1)
Cohort 2 25 mg/m^2	4	77	M	Oral Cavity	Floor of Mouth	T4a, N0	Y	Y	44.5	Composite Resection with ND and FF	--
	5	40	M	Oral Cavity	Lateral Tongue	T2, N1	N	N	59.0	Partial Glossectomy with ND and FF	--
	6	69	F	Lip	Neck Metastasis	T0, N3	N	N	45.5	Composite Resection with ND and FF	Dizziness (Grade 1), ECG Changes (Grade 1), Tumor Pain (Grade 1), Hypomagnesemia (Grade 1)
	7	69	F	Oral Cavity	Buccal Mucosa	T2, N1	N	N	52.0	Wide Local Excision with ND and FF	ECG Changes (Grade 1), Elevated AST (Grade 1), Hypomagnesemia (Grade 1)
	8	38	M	Oral Cavity	Lateral Tongue	T4, N2	N	N	45.0	Total Glossectomy with ND and FF	--
	9	64	M	Cutaneous	Neck	T2, N2b	N	N	47.0	Wide Local Excision with ND and FF	--
Cohort 3 62.5 mg/m^2	10	84	F	Nasal Cavity	Septum	T2, N0	N	N	92.5	Rhinectomy with ND and FF	Tumor Burning (Grade 1), Hypotension (Grade 1)
	11	60	M	Oropharynx	Tonsil	T2, N1	N	N	151.25	Tonsillectomy with ND	--
	12	57	M	Oral Cavity	Floor of Mouth	T3, N2	N	N	147.5	Composite Resection with ND and FF	--

n = 12 patients. Neck dissection (ND), Free flap (FF), Aspartate transaminase (AST), Electrocardiogram (ECG)

peutic dose), cohort 2 received 10% of therapeutic dose, and cohort 3 received 25% therapeutic dose (Table 1). No outliers were excluded from the study analysis.

CETUXIMAB-IRDYE800 CONJUGATION

Conjugation of cetuximab-IRDye800 was performed under cGMP conditions, as previously described.[19] Briefly, cetuximab® (ImClone LLC, Eli Lilly and Company, Branchburg, NJ) was concentrated and pH adjusted by buffer exchange to a 10mg/ml solution in 50mM potassium phosphate, pH 8.5. IRDye800CW NHS ester (LI–COR Biosciences, Lincoln NE) was conjugated to cetuximab for 2hr at 20°C in the dark, at a molar ratio of 2.3:1.

OPTICAL IMAGING

Wide-field near-infrared (NIR) imaging: Routine imaging of the tumor, cervical skin, and forearm skin was performed in the clinic on day 0 and 1 post cetuximab-IRDye800 infusion using a wide-field optical imaging device (Luna Imaging System, Novadaq, Toronto, Canada) designed for intraoperative imaging of indocyanine-green (ICG). For surgical imaging, the protocol stipulated that the imaging data would not be used to guide the surgical procedure. Routine intraoperative equipment was used. The existing equipment could easily be wheeled into the OR and requires mere minutes to acquire fluorescence imaging. The tumor was imaged using the wide-field system prior to resection and ex vivo at post-resection. The wound bed was also imaged after removal of tumor and margins. During wide-field acquisition, video (30s at 7.5f/s and 1/15s or 1/4s integration) of specimen in field of view (30cm or 15cm from camera) was collected at each time-point. Quantitative analysis was performed using integrated instrument software (SPY-Q, Novadaq). Relative fluorescent units (RFU) were measured for tumor and background (area surrounding tumor) and averaged among six individual frames per imaging time-point. Tumor-to-background ratio (TBR) was calculated by dividing tumor RFU by respective background RFU as described previously.[13] For qualitative analysis, exported DICOMs were used to produce videos and images in SPY-Q using standardized threshold values.

Closed-field NIR imaging: The Pearl Impulse imaging platform (LI–COR Biosciences, Lincoln, NE) was used to image fresh tissues obtained in the operating room prior to paraffin embedding. For cohort 1 (2.5mg/m^2), there were three primary tumors resected from three patients yielding 42 bread-loafed specimens. Multiple wound-bed margins (n=27), muscle (n=6), and skin samples (n=6) were also collected and imaged. In cohort 2 (25mg/m^2), there were four primary tumors were imaged from three patients yielding 46 individual specimens. Imaging was also performed on the wound-bed margins (n=26), muscle (n=6), and skin (n=6) sam-

ples. In cohort 3 (62.5mg/m^2), there were three primary tumors from three patients yielding 22 individual specimens. Imaging was also performed on the wound-bed margins (n=12), muscle (n=6), and skin (n=6) samples. Only one intraoperative frozen margin, produced in cohort 3 by patient 12, was histologically-confirmed positive for disease. Tissue thickness of fresh tissue samples was maintained at 4–5mm to normalize for attenuation. For quantitative analysis, mean fluorescent intensity (MFI), defined as total counts/region of interest (ROI) pixel area, was calculated using custom ROI generated for each specimen using integrated instrument software (ImageStudio, LI–COR Biosciences).

HISTOLOGICAL ASSESSMENT

Routine H&E staining was done for histological assessment performed by a board-certified pathologist and then correlated with fluorescence intensity. The Odyssey imaging platform (LI–COR Biosciences) was used to determine fluorescence in slide-mounted sections obtained from paraffin-embedded blocks. To quantify the fluorescence signal, ROIs were drawn in the tumor region (determined by pathologist) and compared with fluorescence of adjacent normal tissue and muscle from remote sites (collected during standard-of-care surgery). This was repeated in three tumor-containing areas of the same slide resulting in an average MFI for each specimen. Immunohistochemistry on unstained tissue sections of tumor, normal, and muscle was performed to evaluate EGFR expression (anti–EGFR Ab–10, Thermoscientific, Waltham, MA) and tumor density (anti-pan Cytokeratin Ab-961, Abcam, Cambridge, MA). Stained slides were imaged using the Bioimagene (Ventana Medical Systems, Tucson, AZ) optical scanner.

ADVERSE EVENTS

Adverse events were classified according to the National Cancer Institute Common Terminology Criteria (Version 4.0). Plasma chemistry profiles (sodium, potassium, chloride, magnesium, calcium, BUN, creatinine, phosphorus, albumin, alkaline phosphatase, ALT, AST, total bilirubin, total protein) for analysis were obtained up to 14 days before surgery and at the following time points: day 0, day 3–4 (date of surgery) and as needed for adverse event assessment. Complete blood count with differential and platelets were obtained at baseline along with coagulation lab values and thyroid stimulating hormone. General physical exam and Karnofsky performance status were assessed prior to enrollment and at days 0, 1, 3–4 (date of surgery), 15, and 30. Adverse events were recorded for up to 30 days beyond the infusion of cetuximab-IRDye800.

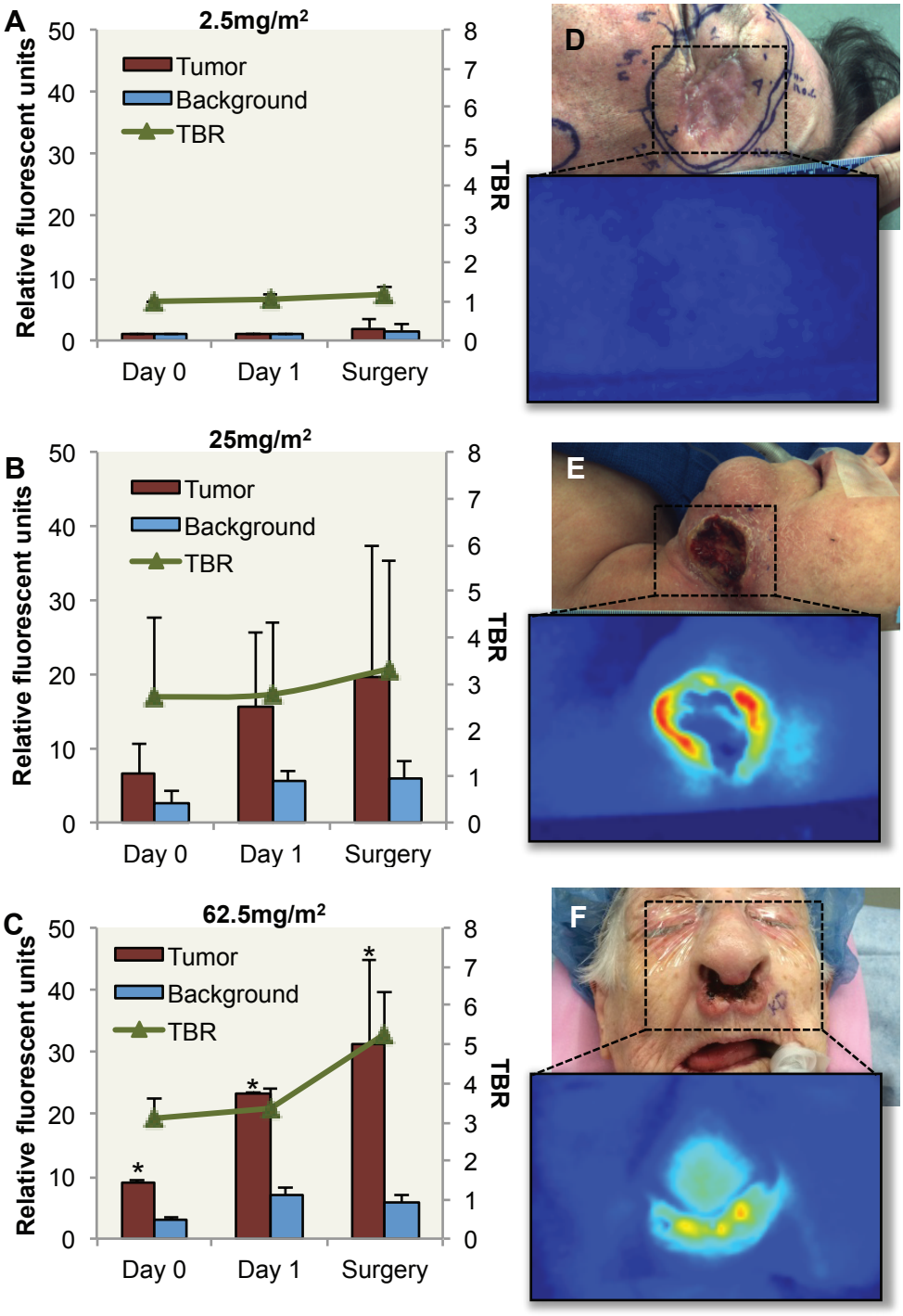
A
2.5mg/m2
Relative fluorescent units
TBR
Tumor
Background
TBR
Day 0
Day 1
Surgery
D
B
25mg/m2
Relative fluorescent units
TBR
Tumor
Background
TBR
Day 0
Day 1
Surgery
E
C
62.5mg/m2
Relative fluorescent units
TBR
Tumor
Background
TBR
Day 0
Day 1
Surgery
F

< Figure 2 Quantification of wide-field fluorescence imaging. *Relative fluorescent units (RFU) acquired during wide-field fluorescent imaging of tumor, background and tumor-to-background ratio (TBR) are shown for (a) 2.5mg/m^2 cohort, (b) 25mg/m^2 cohort, and (c) 62.5mg/m^2 cohort. White light and fluorescence images acquired using wide-field imaging device are shown for (d) 2.5mg/m^2 cohort, (e) 25mg/m^2 cohort, and (f) 62.5mg/m^2 cohort. Asterisk denotes significant (p<0.05) increase in tumor RFU compared to background for respective day. Data are RFU and TBR ± SD.2*

STATISTICAL ANALYSIS

The biostatistician examined the data graphically and calculated descriptive statistics for variables of interest. Differences in fluorescence by tissue type (cancerous versus normal margins; and cancerous versus distal muscle) were tested separately for each dose. Because patients contributed multiple tissue samples and some measurements of cancerous and normal margin fluorescence were made on the same histologic slide, formal testing of differences was done with linear mixed models, incorporating patients and slides as random effects and accounting for the nesting of slides within patients. Descriptive statistics and graphical summaries were done using SAS, SPSS, Excel, and R v 3.0.1. Mixed modeling was done using the lme4 package in R.

RESULTS

PATIENTS AND SAFETY DATA

There were 14 patients who met study criteria, of which two had an infusion reaction to an unlabeled cetuximab test dose prior to receiving cetuximab-IRDye800 and were not enrolled. There were 12 patients (Table 1) who received the study drug; three at the 2.5mg/m^2 and 62.5mg/m^2 dose, and six at the 25mg/m^2 dose. All patients had biopsy proven squamous cell carcinoma originating in the head and neck. There were no grade-2 or higher adverse events attributable to cetuximab-IRDye800 and four possibly related grade-1 adverse reactions occurred in the first cohort, seven in the second cohort, and two in the third cohort (Table 1). Most common adverse events included tumor-site symptoms (n=4) and cardiovascular-related findings (n=4). Patient-specific adverse events are listed in Table 1. Although sample size was limited, at no time point did paired t-tests indicate that the mean QTc was significantly prolonged compared to baseline, either overall or within each cohort (smallest P = 0.10). Also, graphical examination of changes in QTc over time did not suggest a coherent pattern of prolongation. As shown in Supplementary Figure S1A, the total plasma concentration of cetuximab-IRDye800 for 25mg/m^2 was significantly (P<0.05) greater than the 2.5mg/m^2 total plasma concentration at each time point. Additionally, the total plasma concentration for the 62.5mg/m^2 was significantly (P<0.05) greater than the 25mg/m^2 total plasma concentration at each time point. For all doses, the calculated half-life for the study drug was: 25hr in

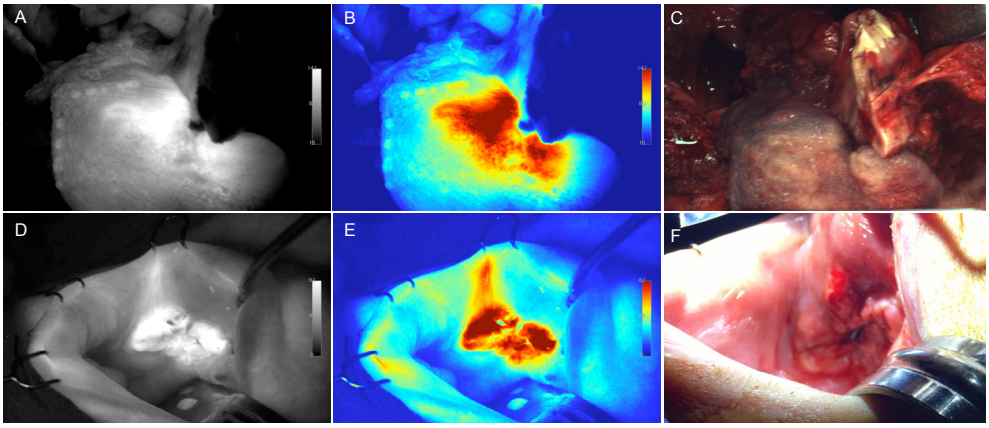

Figure 3 Intraoperative fluorescence imaging. *Shown are (A,D) grayscale fluorescence, (B,E) color map fluorescence, and (C,F) corresponding brightfield acquired using the wide-field device prior to primary tumor resection from patients in the 25mg/m2 dose group undergoing a total glossectomy (A-C) and a wide local excision of the buccal mucosa (D-F).*

cohort 1, 24hr in cohort 2, and 32hr in cohort 3 (Supplementary Fig. S1A). Fluorescent gel electrophoresis also confirmed that the antibody-dye bioconjugate remained intact in serum (Supplementary Fig. S1B).

CLINICAL AND OPERATIVE FLUORESCENCE IMAGING

Wide-field NIR imaging (Luna Imaging System, Novadaq, Toronto, Canada) was performed post-cetuximab-IRDye800 infusion on day 0, 1, and the day of surgical resection. As shown in Fig. 2A, limited fluorescent signal was detectable by wide-field imaging above background in the first cohort (microdose level, 2.5mg/m^2). In patients receiving 25mg/m^2 and 62.5mg/m^2, quantitative analysis of wide-field imaging revealed significantly ($P<0.05$) greater fluorescence detected in the tumor compared to surrounding normal tissue at each imaging time point (Fig. 2B, C). TBR was also shown to improve from day 1 to surgery with an average TBR increase of 2.2 for cohort 3. Representative images of white light and fluorescence are shown in Fig.2d–f for respective patients at each cohort on surgery day. Fluorescence imaging of the primary tumor in situ demonstrated fluorescence with an average TBR of 4.3 (2.1 – 7.8) for cohort 2 and an average TBR of 5.2 (4.8 – 6) for cohort 3.

FLUORESCENCE IMAGING OF PRIMARY TUMOR RESECTION

During the trial, intraoperative imaging of the primary tumor prior to resection was performed using the wide-field device. As shown in Figure 3, grayscale (Fig. 3A, D) and color (Fig. 3B, E) fluorescence imaging provided robust contrast between tumor and surrounding tissues during near-total glossectomy (Fig. 3C) and wide local excision (Fig. 3F) procedures

from the 25mg/m^2 dose group. Quantitative analysis revealed TBR values of 3.2 for Figure 3A-B and 4.1 for Figure 3D-E. The intraoperative imaging performed in these cases is shown in Supplementary Video 1, 2.

CORRELATION OF FLUORESCENCE WITH HISTOLOGICAL DISEASE

To evaluate relationship between fluorescence intensity and tumor deposition, wide-field fluorescence imaging and pathological processing of the primary specimen was mapped to histology (Fig.4). Closed-field fluorescence imaging of freshly processed, whole tissue sections (4-5mm thick, mapped with roman numerals) was performed and fluorescence intensity was shown to correlate with disease areas as determined by board-certified pathologist using H&E stain (marked with black dotted line in adjacent histological sections). The tumor border is clearly visualized using fluorescence, which correlates with disease border during H&E analysis.

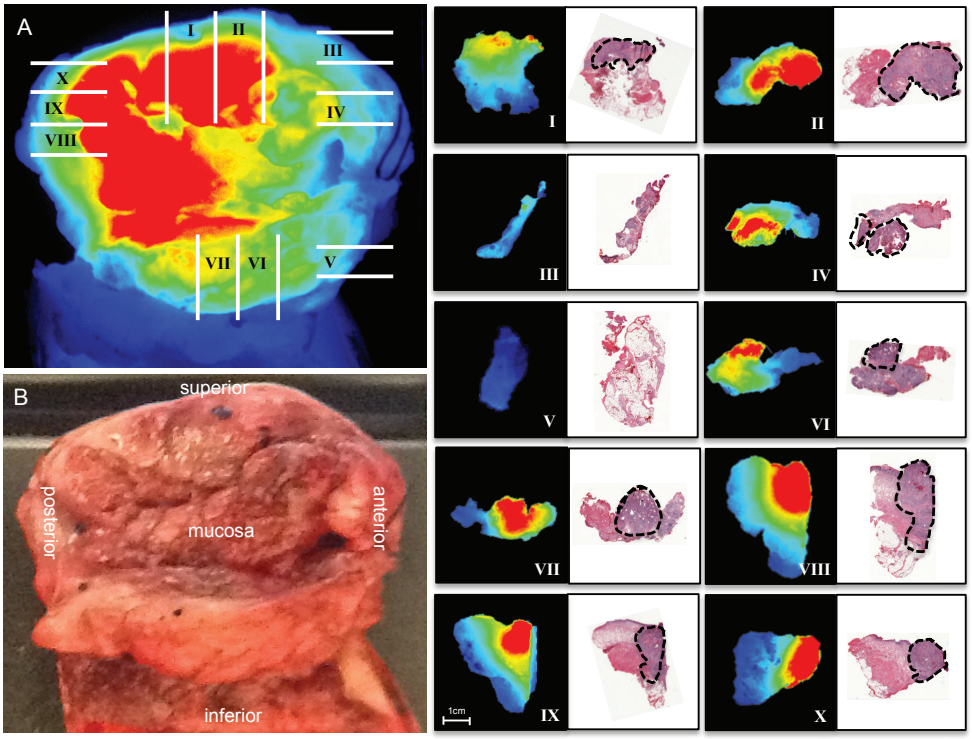

Figure 4 Correlation of fluorescence and disease margin. *Wide-field fluorescence (A) and brightfield (B) image are shown of resected primary tumor. Gridlines represent whole tissue (4-5mm) sections cut during pathological processing of specimen. Breadloaf sections were fluorescently imaged using closed-field imaging device, then formalin-fixed, sectioned, and H&E stained. Black outline represents tumor deposition as determined by board-certified pathologist. Fluorescent images of whole tissue sections and corresponding H&E stained sections are oriented with mucosal side at top.*

TUMOR MAPPING EX VIVO

Tumor mapping of the surgical specimen was performed ex vivo with a closed-field NIR imaging system, the Pearl Impulse (LI–COR Biosciences, Lincoln, NE). Localization of IRDye800 fluorescence in freshly resected tissue prior to paraffin embedding was performed to determine the ability of tumor fluorescence to differentiate tumor from normal tissues and identification of positive margins. To achieve this we first performed a quantitative comparison of MFI from bread-loafed tissue specimens was performed (Fig. 5A) to validate the preferential uptake of IRDye800 fluorescence in cancer tissue. Fluorescence in histologically confirmed tumor tissue was significantly greater ($P<0.001$) than negative epithelial margins, muscle, and skin for each dose. Using peripheral histologically confirmed negative margins to represent background, the calculated TBR for cohort 2 (9.5) was significantly ($P<0.05$) higher than the TBR for both cohort 1 (5.9) and cohort 3 (5.7). Representative white light and fluorescence images are also shown for tumor, margins, skin, and muscle for the 2.5mg/m^2 (Fig. 5B–E), 25mg/m^2 (Fig. 5F–I), and 62.5mg/m^2 (Fig. 5J-M) doses. Although this first in human study was designed not to interfere with standard of clinical care, several observations indicated the clinical benefit of ex vivo tumor fluorescence tumor mapping. In one case the tumor was under-resected and ex vivo fluorescence imaging of tumor margins identified a single deep margin from patient 12 (Supplementary Fig. S2A) in cohort 3 that was pathology-confirmed

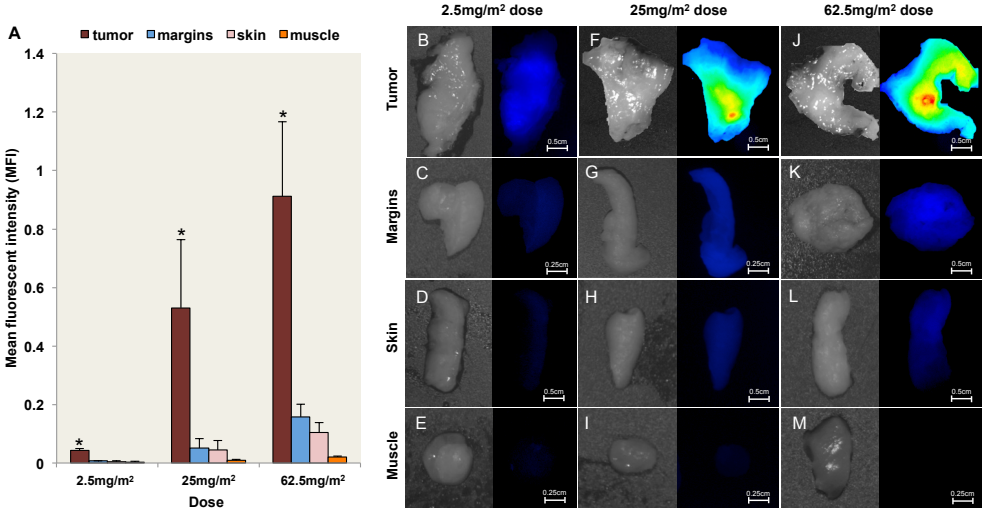

Figure 5 Fluorescent imaging of resected tissues. *(a) Mean fluorescent intensity (MFI) are shown for freshly resected tumor, margin, skin, and muscle for the 2.5mg/m^2, 25mg/m^2, 62.5mg/m^2 dose groups acquired using closed-field imaging system. Representative bright field and fluorescence images of tumor, margins, skin, and muscle are shown for the (b-e) 2.5mg/m^2 dose group, (f-i) 25mg/m^2 dose group, and (j-m) 62.5mg/m^2 dose group. Image scaling was kept consistent for representative images at each dose. Asterisk denotes significant ($p<0.05$) increase in tumor MFI compared to margins, skin, and muscle for respective dose. Scale bars represent 0.5cm or 0.25cm. Data are MFI ± SD.*

positive for cancer during intraoperative frozen section assessment. The relative fluorescent counts of the positive margin were 2-fold higher (Supplementary Fig. S2B) than the negative margins (Supplementary Fig. S2C-E) when imaged using the wide-field, intraoperative instrument. In another patient the tumor was over resected; the surgeon committed to the resection margin (Supplementary Fig. S3A) prior to optical imaging. Post-resection optical imaging (Supplementary Fig. S3B, brightfield) of a primary cutaneous squamous cell carcinoma from cohort 1 (2.5mg/m^2 dose) demonstrated that the surgical margin, as determined by pathological assessment, extended significantly (greater than 3 cm) beyond the optical margin, which was also predicted using closed-field (Supplementary Fig. S3C) and wide-field (Supplementary Fig. S3D) imaging. In this case, the surgical margins were overestimated by the surgeon based on non-specific changes associated with previous surgery and radiation in this patient. Unfortunately, in the current study, inadequate number of positive margins prohibited statistical analysis.

MOLECULAR CORRELATIONS

Because the IRDye800 survives pathological processing and can be localized with high resolution in unstained paraffin sections, fluorescence intensity was correlated with the presence of histologically confirmed tumor, normal adjacent tissue, or muscle containing areas. In Fig. 6A, a representative H&E stain is shown from the 25mg/m^2 dose. Areas of tumor and normal tissue, as determined by board-certified pathologist, are annotated. Regions that were histologically positive for tumor were found to have significantly ($P<0.001$) higher fluorescence compared to normal tissue (Fig. 6B). Furthermore, univariate analysis within all doses showed a strong correlation ($P<0.001$) with EGFR expression (Fig. 6C) and tumor density ($P<0.05$). In multivariate models, EGFR expression remained significantly associated with fluorescence intensity ($P<0.001$) but tumor density did not ($P>0.05$). MFI of pathology-positive tumor was significantly greater ($P<0.001$) than normal and muscle for each dose (Fig. 6D). There was no correlation ($P>0.05$) between fluorescence and tumor stage, tumor site, or adverse events.

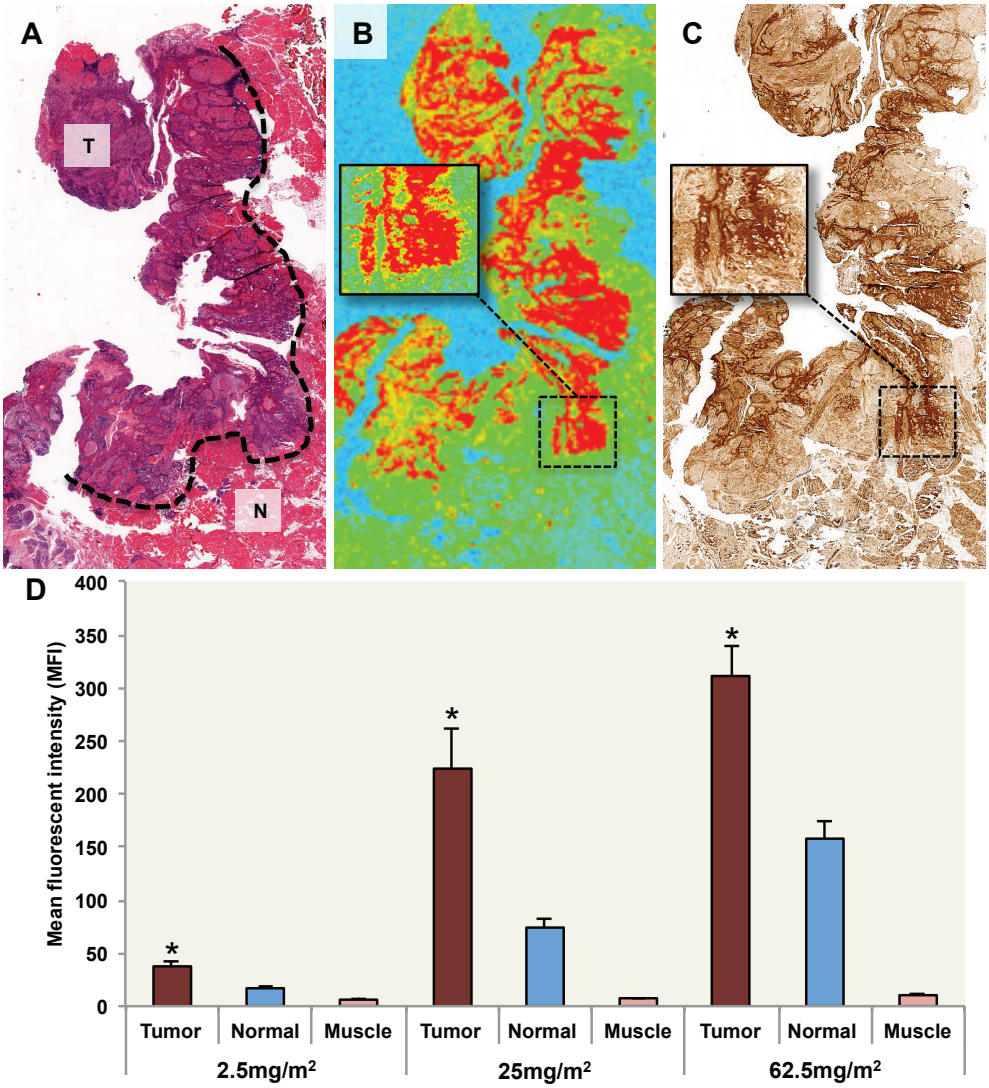

Figure 6 Histopathology and fluorescence localization. *(a) Representative H&E image of tumor sections from the 25mg/m² dose group. Pathology-positive areas of cancer are outlined: T=Tumor, N=Normal adjacent tissue. (b) Fluorescence image of fixed, unstained tumor section shown in panel (a) acquired using fluorescent scanner with inset magnified area of pathology-positive cancer and (c) EGFR stain. (d) Mean fluorescent intensity (MFI) acquired using fluorescent scanning of fixed unstained tissue sections is shown for tumor, normal adjacent, and muscle. Data are MFI ± SE. Asterisk denotes significant (p<0.001) increase in tumor MFI compared to normal and muscle for respective dose.*

DISCUSSION

Successful fluorescent labeling of commercially available antibodies for human use to localize disease with high resolution may represent a unique opportunity in oncologic imaging. We demonstrate for the first time that tumor overexpression of EGFR can be safely exploited for diagnostic imaging and this targeting approach produces tumor-to-background ratio sufficient for surgical decision-making. Several important observations could be made based on this trial data, which will be highly relevant for the field. First, microdosing provides limited contrast and strategies that target tumor receptors should not be constrained to an exploratory approach (Phase 0 trials). Second, tumor mapping ex vivo identified suspicious areas on the specimen and on peripheral margins to reduce sampling error. Third, adverse events of the labeled antibody were consistent with the known toxicity profile of unlabeled cetuximab. And finally, this optical labeling technique could be safely applied to other protein-based therapeutics to confirm successful targeting or assess off-target activity during early phase trials.

While the current study was a phase 1 safety trial and therefore did not alter the standard of care, the disease margin was correlated with the fluorescence margin generated from specific probe emission where feasible and examples of this process are provided. In figure 4, the pathological processing was registered with the whole specimen image and then correlated with the histopathological-determined disease margin, which is annotated in the adjacent H&E image. As shown in figure 6, this degree of correlation was also performed at the microscopic level with representative H&E images of tumor sections from the 25mg/m^2 dose group. Additionally, the supplementary intraoperative videos and figure 3 images demonstrate the level of real-time resolution afforded when using the fluorescence information compared to the adjacent brightfield images, which serve as current standard of care.

Systemic administration of cetuximab-IRDye800 had grade-1 toxicities in each cohort that occurred in a dose independent manner. Fluorescent imaging using a wide-field, intraoperative device could differentiate tumor from normal tissue with an average TBR of 5.2 in the higher dose range. Over the 3–4 days post-infusion, a gradual increase in TBR was visible over time, suggesting that achieving peak TBR may require longer periods between infusion and surgical intervention, which is consistent with preclinical data.[14,20] Tumor EGFR expression was strongly associated with fluorescence intensity and was an independent predictor of fluorescence when compared to tumor density. As a first in human trial, the protocol was designed not to alter the standard of care, however, in this limited study opportunities were identified to improve delivery of surgical ablation and pathological processing.

As a dose ranging study, the results support the middle dose of 25mg/m^2. Evidence of receptor saturation at the highest dose was demonstrated among each imaging platform. For wide-field imaging, which would guide intraoperative decision making, there was no significant difference in TBR between the 25mg/m^2 and 62.5mg/m^2 doses (4.3 to 5.2, respectively). For the closed-field system imaging, which was performed for fluorescence guided tumor mapping to validate tumor localization of IRDye800, the TBR was highest in the 25mg/m^2 group (9.9) versus the 2.5mg/m^2 group (5.9) and the 62.5mg/m^2 group (5.7). When slide-mounted sections were imaged for fluorescence, the TBR (determined using MFI values from pathology positive tumor and adjacent normal areas) was highest for the 25mg/m^2 group (2.9) compared to the 2.5mg/m^2 (2) and 62.5mg/m^2 groups (1.7). Due to the loss in optimal TBR associated with the highest dose, the 25mg/m^2 cetuximab-IRDye800 dose was considered optimal among the nine patients evaluated.

Although this is the first in human use of fluorescently labeled antibodies for detection of microscopic disease, tumor-specific optical imaging has been applied in humans for surgical navigation of gliomas[21,22] and ovarian cancer.[23] The use of 5–ALA for glioma surgery has advanced to phase 3 clinical trials where it was shown to improve oncologic and functional outcomes.[5] Although 5–ALA imaging has significant limitation for application outside of glioma surgery (dependent on a high tumor metabolic rates, possesses wavelengths with sub-optimal tissue penetration), approval in Europe and subsequent studies have demonstrated that fluorescence-based surgical navigation can improve outcomes. The only other in human study was administration of folate-fluorescein agent, which was shown to identify metastatic peritoneal disease in three out of ten patients tested.[24] Tumor detection was limited to patients with peritoneal metastasis with high folate receptor expression.

Labeling cetuximab with IRDye800 as an oncologic contrast agent has several unique advantages including the ability to image multiple cancer types and develop other antibodies for optical imaging. The known pharmacokinetics can be applied to manufacturing and trial design to achieve cost-effective and safe clinical translation. Furthermore, use of an optical dye with excitation and emission wavelengths that overlap with ICG allows access to a large pool of existing intraoperative imaging devices for early-phase trials, which can reduce cost of widespread adoption of this technology.[19] Clinical translation of novel probes has been limited because development of imaging agents is expensive, toxicities are unknown, and there is limited expected return compared to therapeutic agents. Although the long half-life of antibodies may result in increased background several days following administration, the long circulating times may also increase cellular incorporation thereby achieving higher tu-

mor penetration over time compared to normal tissues.[25,26] Despite the spectrum of targeting vectors proposed in preclinical studies, therapeutic antibodies applied to diagnostic purposes might provide the most straightforward path to the clinic.

Here we demonstrate for the first time that antibodies can be fluorescently labeled for high resolution of identification of cancer for clinical application. We show that cetuximab-IRDye800 can be safely administered as a tumor-specific contrast agent, which may be helpful for surgical navigation to identify subclinical disease in EGFR-expressing tumors. Fluorescently labeled therapeutic antibodies may also be valuable to measure tumor-specific uptake, pharmacokinetics, and biodistribution in early phase clinical trials of these agents. Furthermore, high-resolution localization of antibody-dye conjugates within tumor tissues (stroma, vasculature, and cancer cells) and within the cell using confocal microscopy may provide novel methodology for determining patients likely to respond to antibody-based therapeutics.

ACKNOWLEDGEMENTS

This work was supported by the Robert Armstrong Research Acceleration Fund, the UAB Comprehensive Cancer Center and NIH/NCI (R21CA182953, R21CA179171, T32CA091078), and institutional equipment loans from Novadaq and LI–COR Biosciences. The authors report no conflict of interest.

SUPPORTING INFORMATION

Additional supporting information may be found in the online version of this article:

Supplementary Figure S1 Pharmacokinetics of cetuximab-IRDye800

Supplementary Figure S2 Fluorescent imaging of positive margin using intraoperative instrument

Supplementary Figure S3 Opportunity for tissue saving procedures

Supplementary Video S1

REFERENCES

1. Arbes SJ Jr, Olshan AF, Caplan DJ, Schoenbach VJ, Slade GD, Symons MJ. Factors contributing to the poorer survival of black Americans diagnosed with oral cancer (United States). Cancer Causes Control. 1999 Dec;10(6):513-23.
2. Woolgar JA, Triantafyllou A. A histopathological appraisal of surgical margins in oral and oropharyngeal cancer resection specimens. Oral Oncol. 2005 Nov;41(10):1034-43.
3. McMahon J, O'Brien CJ, Pathak I, Hamill R, McNeil E, Hammersley N, Gardiner S, Junor E. Influence of condition of surgical margins on local recurrence and disease-specific survival in oral and oropharyngeal cancer. Br J Oral Maxillofac Surg. 2003 Aug;41(4):224-31.
4. Hinni ML, Ferlito A, Brandwein-Gensler MS, Takes RP, Silver CE, Westra WH, Seethala RR, Rodrigo JP, Corry J, Bradford CR, Hunt JL, Strojan P, Devaney KO, Gnepp DR, Hartl DM, Kowalski LP, Rinaldo A, Barnes L. Surgical margins in head and neck cancer: a contemporary review. Head Neck. 2013 Sep;35(9):1362-70.
5. Stummer W, Pichlmeier U, Meinel T, Wiestler OD, Zanella F, Reulen HJ; ALA-Glioma Study Group. Fluorescence-guided surgery with 5-aminolevulinic acid for resection of malignant glioma: a randomised controlled multicentre phase III trial. Lancet Oncol. 2006 May;7(5):392-401.
6. Stummer W, Novotny A, Stepp H, Goetz C, Bise K, Reulen HJ. Fluorescence-guided resection of glioblastoma multiforme by using 5-aminolevulinic acid-induced porphyrins: a prospective study in 52 consecutive patients. J Neurosurg. 2000 Dec;93(6):1003-13..
7. Stummer W, Reulen HJ, Novotny A, Stepp H, Tonn JC. Fluorescence-guided resections of malignant gliomas--an overview. Acta Neurochir Suppl. 2003;88:9-12.
8. Millesi M, Kiesel B, Woehrer A, Hainfellner JA, Novak K, Martínez-Moreno M, Wolfsberger S, Knosp E, Widhalm G. Analysis of 5-aminolevulinic acid-induced fluorescence in 55 different spinal tumors. Neurosurg Focus. 2014 Feb;36(2):E11. Millesi M, Kiesel B, Woehrer A, Hainfellner JA, Novak K, Martinez-Moreno M, et al. Analysis of 5-aminolevulinic acid-induced fluorescence in 55 different spinal tumors. Neurosurgical focus. 2014;36:E11.
9. Taruttis A, Ntziachristos V. Translational optical imaging. AJR Am J Roentgenol. 2012 Aug;199(2):263-71.
10. Thurber GM, Figueiredo JL, Weissleder R. Multicolor fluorescent intravital live microscopy (FILM) for surgical tumor resection in a mouse xenograft model. PLoS One. 2009 Nov 30;4(11):e8053.
11. Hall MA, Pinkston KL, Wilganowski

N, Robinson H, Ghosh P, Azhdarinia A, Vazquez-Arreguin K, Kolonin AM, Harvey BR, Sevick-Muraca EM. Comparison of mAbs targeting epithelial cell adhesion molecule for the detection of prostate cancer lymph node metastases with multimodal contrast agents: quantitative small-animal PET/CT and NIRF. J Nucl Med. 2012 Sep;53(9):1427-37.

12. Mitsunaga M, Tajiri H, Choyke PL, Kobayashi H. Monoclonal antibody-fluorescent probe conjugates for in vivo target-specific cancer imaging: toward clinical translation. Ther Deliv. 2013 May;4(5):523-5.
13. Heath CH, Deep NL, Sweeny L, Zinn KR, Rosenthal EL. Use of panitumumab-IRDye800 to image microscopic head and neck cancer in an orthotopic surgical model. Ann Surg Oncol. 2012 Nov;19(12):3879-87.
14. Day KE, Beck LN, Deep NL, Kovar J, Zinn KR, Rosenthal EL. Fluorescently labeled therapeutic antibodies for detection of microscopic melanoma. Laryngoscope. 2013 Nov;123(11):2681-9.
15. Ang KK, Berkey BA, Tu X, Zhang HZ, Katz R, Hammond EH, Fu KK, Milas L. Impact of epidermal growth factor receptor expression on survival and pattern of relapse in patients with advanced head and neck carcinoma. Cancer Res. 2002 Dec 15;62(24):7350-6.
16. Rubin Grandis J, Melhem MF, Gooding WE, Day R, Holst VA, Wagener MM, Drenning SD, Tweardy DJ. Levels of TGF-alpha and EGFR protein in head and neck squamous cell carcinoma and patient survival. J Natl Cancer Inst. 1998 Jun 3;90(11):824-32.
17. Suh Y, Amelio I, Guerrero Urbano T, Tavassoli M. Clinical update on cancer: molecular oncology of head and neck cancer. Cell Death Dis. 2014 Jan 23;5:e1018.
18. Marshall MV, Draney D, Sevick-Muraca EM, Olive DM. Single-dose intravenous toxicity study of IRDye 800CW in Sprague-Dawley rats. Mol Imaging Biol. 2010 Dec;12(6):583-94.
19. Zinn KR, Korb M, Samuel S, Warram JM, Dion D, Killingsworth C, Fan J, Schoeb T, Strong TV, Rosenthal EL. IND-directed safety and biodistribution study of intravenously injected cetuximab-IRDye800 in cynomolgus macaques. Mol Imaging Biol. 2015 Feb;17(1):49-57.
20. Korb ML, Hartman YE, Kovar J, Zinn KR, Bland KI, Rosenthal EL. Use of monoclonal antibody-IRDye800CW bioconjugates in the resection of breast cancer. J Surg Res. 2014 May 1;188(1):119-28.
21. Li Y, Rey-Dios R, Roberts DW, Valdés PA, Cohen-Gadol AA. Intraoperative fluorescence-guided resection of high-grade gliomas: a comparison of the present techniques and evolution of future strategies. World Neurosurg. 2014 Jul-Aug;82(1-2):175-85.
22. Roberts DW, Valdés PA, Harris BT, Har-

tov A, Fan X, Ji S, Leblond F, Tosteson TD, Wilson BC, Paulsen KD. Glioblastoma multiforme treatment with clinical trials for surgical resection (aminolevulinic acid). Neurosurg Clin N Am. 2012 Jul;23(3):371-7.

23. van Dam GM, Themelis G, Crane LM, Harlaar NJ, Pleijhuis RG, Kelder W, Sarantopoulos A, de Jong JS, Arts HJ, van der Zee AG, Bart J, Low PS, Ntziachristos V. Intraoperative tumor-specific fluorescence imaging in ovarian cancer by folate receptor-α targeting: first in-human results. Nat Med. 2011 Sep 18;17(10):1315-9.
24. van Dam GM, Themelis G, Crane LM, Harlaar NJ, Pleijhuis RG, Kelder W, Sarantopoulos A, de Jong JS, Arts HJ, van der Zee AG, Bart J, Low PS, Ntziachristos V. Intraoperative tumor-specific fluorescence imaging in ovarian cancer by folate receptor-α targeting: first in-human results. Nat Med. 2011 Sep 18;17(10):1315-9.
25. Thurber GM, Dane Wittrup K. A mechanistic compartmental model for total antibody uptake in tumors. J Theor Biol. 2012 Dec 7;314:57-68.
26. Wittrup KD, Thurber GM, Schmidt MM, Rhoden JJ. Practical theoretic guidance for the design of tumor-targeting agents. Methods Enzymol. 2012;503:255-68.